Journal of Electrochemistry

Volume 20
Issue 3 *Special Issue on Fundamental Electrochemistry(Editor: Professor CHEN Sheng-li)*

2014-06-28

Effects of Oxygen Coverage and Hydrated Proton Model on the DFT Calculation of Oxygen Reduction Pathways on the Pt(111) Surface

Li-hui OU

Sheng-li CHEN
College of Chemistry and Molecular Sciences, Wuhan University, Wuhan 430072, China;,
slchen@whu.edu.cn

Recommended Citation
Li-hui OU, Sheng-li CHEN. Effects of Oxygen Coverage and Hydrated Proton Model on the DFT Calculation of Oxygen Reduction Pathways on the Pt(111) Surface[J]. *Journal of Electrochemistry*, 2014 , 20(3): 206-218.
DOI: 10.13208/j.electrochem.130894
Available at: https://jelectrochem.xmu.edu.cn/journal/vol20/iss3/3

DOI: 10.13208/j.electrochem.130894 **Artical ID**:1006-3471(2014)03-0206-13
Cite this: *J. Electrochem.* **2014**, *20*(3): 206-218 **Http**://electrochem.xmu.edu.cn

Effects of Oxygen Coverage and Hydrated Proton Model on the DFT Calculation of Oxygen Reduction Pathways on the Pt(111) Surface

OU Li-hui[1,2], CHEN Sheng-li[2*]
(1. *College of Chemistry and Chemical Engineering, Hunan University of Arts and Science, Changde* 415000, *Hunan, China;* 2. *College of Chemistry and Molecular Sciences, Wuhan University, Wuhan* 430072, *China*)

Abstract: DFT calculation is used to study various possible steps in the oxygen reduction reaction (ORR), including the adsorption and dissociation process of O_2 and the serial protonation process of dissociated products to form H_2O on the Pt(111) surface. By using slabs of different sizes, and different numbers of pre-adsorbed oxygen atoms, the coverage effects on the pathways are investigated. The calculated results using different hydrated proton models are also compared. It is shown that the initial step of the ORR is the formation of a protonated end-on chemisorbed state of OOH*, which can transform to an unprotonated top-bridge-top state of O_2* or dissociate into adsorbed O* species with similar activation barrier. The calculated activation barriers for various possible steps at different oxygen coverages suggest that the protonation of O* to form OH* species is the rate-determining step in the ORR. With the increased oxygen coverage, the activation energy of this step decreases. It is found that the use of hydrated proton models more complicated than $H_7O_3^+$ does not change the calculated pathways.

Key words: minimum energy path; ORR mechanism; oxygen coverage; hydrated proton model
CLC Number: O646 **Document Code**: A

The oxygen reduction reaction (ORR) has long been a model reaction in electrocatalysis. In the mean time, as the cathode reaction in the fuel cells, its sluggish kinetics has become one of the major bottlenecks for improving the efficiency of fuel cells[1-4]. Pt is so far the best ORR catalyst among various metals. Understanding the ORR mechanism and kinetics on the Pt electrode surfaces is of great significance in designing efficient cathode catalysts for fuel cells. Therefore, the ORR on the Pt surfaces has been a research focus of recent experimental and theoretical studies[1-12].

Despite of extensive studies during the last a few decades, the atomic level mechanism of the ORR on Pt is still unclear in several aspects. Earlier experimental studies of the ORR on Pt electrodes in acid solutions exhibited a reaction order of ca. 1.0 with respect to O_2 and a Tafel slope of ca. 120 mV·decade^{-1} in the potential range where the Pt surface is practically free of chemisorbed oxygen. Accordingly, the first proton-coupled charge transfer and proton transfer reaction, namely, $O_2 + H^+ + e \rightarrow OOH_{ad}$, was proposed as the rate-determining step (*rds*)[3]. However, the measurement by Neyerlin et al.[4,13-14] using Pt/C catalyst in the cathode of a fuel cell showed that the full description of ORR kinetics in the potential range relevant to fuel cell operation should be based on a

Received: 2014-03-19, Revised: 2014-05-02 *Corresponding author, Tel: (86-27)68754693, E-mail: slchen@whu.edu.cn
This work was supported by Ministry of Science and Technology (Grant Nos. 2012CB932800 and 2013AA110201), the National Natural Science Foundation of China (Grant No. 21303048), Hunan Provincial Natural Science Foundation of China (Grant No. 13JJ4101), and Foundation of the Education Department of Hunan Province (Grant No. 12C0832)

constant Tafel slope of 60 mV·decade^{-1} and a reaction order of 0.5 with respect to oxygen molecule. They therefore conjectured that the *rds* in the ORR may be the electron and proton transfers to the adsorbed hydroxyl (OH_{ads}) or oxygen atom (O_{ads}), namely, $O_{ad} + H^+ + e \rightarrow OH_{ad}$ or $OH_{ad} + H^+ + e \rightarrow H_2O$. Lately, Wang and her colleague[11] analyzed the 4-electron ORR on the Pt(111) surface in an acid medium with an intrinsic kinetic equation using free energies of activation and adsorption as the kinetic parameters. The model fitting to experimental data suggested that the 4-electron ORR on Pt is desorption-limited because the dissociative adsorption is facile, while O and OH are strongly trapped on the surface. Above the reversible potential for the O and OH transition, the O coverage is high, causing severe inhibition of the ORR activity. As O coverage falls with decreasing potential, the kinetic current increases with the lowering the reductive desorption activation barrier and increasing OH coverage. Thus, ORR mechanism is strongly coverage-dependent.

In recent years, the *ab initio* calculations become a necessary and valuable alternative for unveiling the molecular mechanism of the ORR due to the essential inaccessibility of electrode/electrolyte interface to low temperature and ultrahigh vacuum conditions using various surface science techniques. Based on density functional theory (DFT) calculations, the ORR pathways including the adsorption and dissociation of O_2 were first investigated by Anderson and his colleagues[5] with a dual-Pt-atom cluster representing the electrode and a hydrated hydronium cluster of $H_7O_3^+$ to model the acidic solution, and by Hyman and Medlin[6] who used a Pt(111) periodical slab to model the electrode and a $H_5O_2^+$ cluster to model the acid solution. These two studies both showed that top-bridge-top adsorption between two Pt atoms is the most favored adsorption state for O_2 in the presence of hydrated hydronium ion, which seemed to support Yeager's proposition[12] that bridge molecular adsorption is necessary for the direct 4-electron reduction of O_2. These theoretical calculations suggested different *rds* for the ORR, namely, the formation of OOH[5] and the dissociation of OOH*[6]. The *ab initio* molecular dynamic (MD) simulations using a $H_7O_3^+$ hydronium cluster as the proton model by Wang and Balbuena[7] showed that the proton transfer occurs accompanying the adsorption of O_2 molecule, forming an end-on OOH* intermediate which can dissociate with negligible activation barrier. However, the research results have shown that the Pt-based alloy catalysts binding atomic oxygen more weakly have better ORR activity, which seemingly can not be well accounted for the views that the *rds* of ORR is the formation of OOH* or its dissociation.

Recent DFT calculation studies on the ORR have been focused on treatments of the potential and solvent. By incorporating more complicated solvent model, the DFT calculations by Yao et al.[15] showed that the OH formation is the *rds* in Pt-catalyzed ORR, whereas the results by Nørskov et al. suggested that the process of OH reduction to H_2O molecule is the potential determining step for ORR using DFT calculations[16]. In the meantime, the DFT-calculated results by Yao et al. also showed that the barrier of *rds* is oxygen-coverage dependent, and the barrier decreases as oxygen increases[17]. Recent *ab initio* calculations studies of ORR by Neurock et al.[18] and by Liu et al.[19] are also worthwhile to mention. In these two studies, the authors have attempted to incorporate the influence of electrode potential in DFT calculations on the activation barriers of possible steps in ORR by adding charge to reaction systems. The optimal electrochemical reaction paths were determined kinetically under the specific electrode potential, in which the proton-coupled O—O bond breaking, i.e. $H^+ + e + O_{2ad} \rightarrow O_{ad} + OH_{ad}$ channel, is identified as the major mechanism for ORR on Pt catalyst.

Despite numerous theoretical studies, the detailed electrocatalytic mechanisms for ORR on the Pt(111) surface remains unclear and various conclusions have been drawn in different studies. It remains a great challenge so far for electrochemists to formulate the entire steps for Pt-catalyzed ORR due to a number of key questions that remain. In the existing theoretical

calculation studies on ORR mechanisms, different solvation and hydrated proton models have been used to mimic an acid medium, which may affect the calculated results. Additionally, the coverage effect of the oxygenated species has not been adequately considered. In present paper, we would like to highlight the effects of oxygen coverage and hydrated proton model on DFT calculations of ORR pathways through performing detailed calculations on the geometric structural optimization and the minimum energy path analysis, including the adsorption and dissociation process of O_2 and the serial protonation process of dissociated products to form H_2O on the Pt(111) surface. In addition, the effect of solvation is also considered by adding explicit water molecules on hydrated hydronium ion model.

1 Models and Methods

Calculations were performed in the framework of DFT on periodic super-cells, using the generalized gradient approximation (GGA) of Perdew-Burke-Ernzerhof (PBE) functional[20] for exchange-correlation and ultrasoft pseudopotentials[21] for Nuclei and core electrons. The Kohn-Sham orbitals were expanded in a plane-wave basis set with a kinetic energy cutoff of 30 Ry and the charge-density cutoff of 300 Ry. The Fermi-surface effects have been treated by the smearing technique of Methfessel and Paxton, using a smearing parameter of 0.02 Ry[22]. The PWSCF codes contained in the Quantum ESPRESSO distribution were used to implement all calculations[23], while figures of the chemical structures were produced with the XCRYSDEN graphical package[24-26].

In all calculations, we used (2×2) three-layer and (3×3) four-layer fcc(111) slabs with theoretical equilibrium lattice constant of 0.399 nm (Pt) to model the Pt(111) surface, which is well consistent with experimental equilibrium lattice constant of 0.3923 nm (Pt). Brillouin-zone (BZ) integrations were performed with the special-point technique, using (4×4) and (3×3) uniformly shifted k-meshs for (2×2) and (3×3) slabs, respectively. Vacuum layers of 1.6 nm in thickness were added above the top layer of slabs in all cases. The Pt atoms in the bottom two layers were fixed at the theoretical bulk positions, whereas the top layer on (2×2) three-layer slabs and top two layers on (3×3) four-layer slabs were allowed to relax and all the other structural parameters had been optimized so as to minimize the total energy of the system. Structural optimization was performed until the Cartesian force components acting on each atom were brought below 10^{-3} Ry·Bohr^{-1} and the total energy converged to within 10^{-5} Ry with respect to structural optimization.

The climbing image nudged elastic band method (CI-NEB) was employed to locate the saddle points and minimum energy paths (MEPs)[27-28]. The transition state images from the NEB calculations were optimized using the quasi-Newton method, which minimizes the forces to find the saddle point. Geometry optimization was performed for each intermediate point in MEPs, in which the bottom two layers of metal atoms were fixed while the top layer of metal atoms and all other nonmetal atoms were allowed to relax.

2 Results and Discussion

2.1 Adsorption and Dissociation of O_2 in the Presence of Hydrated Proton

1) Effects of O Coverage

The adsorption and dissociation of O_2 on the (2×2)-Pt(111) surface have been investigated by *ab initio* DFT calculations in our previous work using hydronium ion $H_7O_3^+$ as a model of solvated proton in acid solution[29-30]. The results indicated that O_2 first forms a metastable end-on chemisorption state OOH in the presence of hydrated hydronium, which can transform to a stable unprotonated top-bridge-top (t-b-t) molecular chemisorption state or dissociate directly into O and OH species in nearly nonactivated processes. To evaluate the effects of oxygen coverage and hydrated proton model on the DFT calculations of ORR pathways, we investigated first the adsorption and dissociation process of O_2 molecule on the (3×3)-Pt (111) surface in the presence of hydrated hydronium ion $H_9O_4^+$. Similar to the (2×2)-Pt(111)/O_2/$H_7O_3^+$ system, physisorption and two molecular chemisorption (one having a tilted end-on configura-

tion and the other one having a top-bridge-top bridge configuration) states, respectively, were also identified for (3×3)-Pt(111)/O_2/$H_9O_4^+$ system through geometry optimizations (Fig. 1A-C). However, it was found that the dissociation of O_2 formed two adsorbed O atoms at fcc hollow site of Pt surface, rather than an O and an OH as did in (2×2)-Pt(111)/O_2/$H_7O_3^+$ system. This indicated that the oxygen coverage and the model of hydrated hydronium impact the dissociation.

Tab. 1 gives the geometric and energetic parameters for various adsorption states of (3×3)-Pt(111)/O_2/$H_9O_4^+$ system. The corresponding value of (2×2)-Pt(111)/O_2/$H_7O_3^+$ system is also given for comparison. The physisorption state had negligible change in O—O bond length compared with the isolated O_2 molecule, and that the O—O bond length and the distance between Pt and O_2 of two chemisorption states on the (3×3)-Pt (111) surface are consistent with that on the (2×2)-Pt(111) surface. According to the values of the adsorption energy E_{ad}[29-30], the top-bridge-top chemisorption state represents the most stable molecular adsorption state. The energy difference between end-on chemisorption state and the physisorption state is -0.31 eV, and it is -0.57 eV between top-bridge-top chemisorption state and the physisorption state in (2×2)-Pt(111)/O_2/$H_7O_3^+$ system, whereas corresponding energy differences in present system are -0.64 eV and -0.92 eV, respectively. The results showed that the reaction energy between the chemisorption state and the physisorption state is more negative under low oxygen coverage. Based on

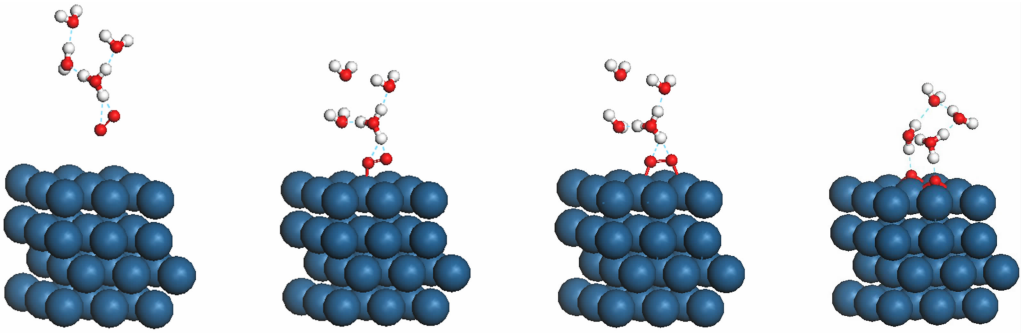

Fig. 1 Various geometric configurations of (3×3)-Pt(111)/O_2/$H_9O_4^+$ system: A. the optimized physisorption state; B. the optimized end-on chemisorption state; C. the optimized top-bridge-top chemisorption state; D. the dissociative atomic chemisorption state

Tab. 1 The geometric and energetic parameters for various adsorption states of (2×2)-Pt(111)/O_2/$H_7O_3^+$ and (3×3)-Pt(111)/O_2/$H_9O_4^+$ systems

System	Adsorption state	$R_{Pt\text{-}O_2}/n$	$R_{O\text{-}O}$/nm	$R_{O\text{-}H}$/nm	E_{ad}/eV
(2×2)-Pt(111)/O_2/$H_7O_3^+$	Physisorption	0.348	0.124	0.210	0
	End-on chemisorption	0.204	0.134	0.131	-0.31
	Top-bridge-top chemisorption	0.194	0.144(0.141)[a]	0.179	-0.57
(3×3)-Pt(111)/O_2/$H_9O_4^+$	physisorption	0.392	0.126	0.150	0
	End-on chemisorption	0.204	0.134	0.134	-0.64
	Top-bridge-top chemisorption	0.195	0.142(0.142)[a]	0.164	-0.92

[a] The values in parenthesis are O—O bond length of top-bridge-top state considering solvent effect, which is consistent in the presence or absence of bilayer structure of H_2O molecule, indicating little solvent effect on geometry structure of chemisorption state

the Brønsted-Evans-Polanyi (BEP) relationship[31], the reaction energy becomes more negative, the activation energy will be predicted to be smaller, which will be validated by a subsequent MEP analysis.

Fig. 2 shows the MEPs for the formation of the most stable top-bridge-top molecular chemisorption state and its dissociation in the (3×3)-Pt(111)/O_2/$H_9O_4^+$ system. It can be seen that the physisorption state is separated from the top-bridge-top chemisorption state by an activation barrier of ca. 0.02 eV, and the subsequent dissociation of the top-bridge-top adsorbed O_2 requires an activation energy of ca. 0.15 eV, both of which are smaller than the value of corresponding process in the (2×2)-Pt(111)/O_2/$H_7O_3^+$ system[29]. These results indicated that the adsorption and dissociation may be more easily to occur under low oxygen coverage.

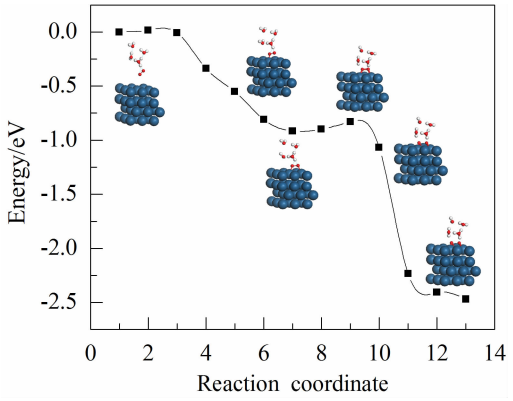

Fig. 2 The minimum energy paths for the transformations from physisorbed O_2 to the chemisorbed molecular O_2 of top-bridge-top configuration and the subsequent dissociation of the top-bridge-top adsorbed O_2 in the presence of hydrated proton $H_9O_4^+$

It can be found in Fig. 2 that there is an end-on adsorbed state in the process of forming top-bridge-top chemisorption state in the (3×3)-Pt(111)/O_2/$H_9O_4^+$ system. Fig. 3 gives more meticulous MEPs for the formation of the most stable top-bridge-top molecular chemisorption state from physisorption state via end-on intermediate. It can be seen that a relatively level region is formed in the middle of the energy path, which is both preceded and followed by a continuous energy falling section, as observed in the (2×2)-Pt(111)/O_2/$H_7O_3^+$ system. The occurrence of such an energy plateau in MEP infers that a relatively stable intermediate state is involved in course of the formation of top-bridge-top chemisorption state on the (3×3)-Pt(111) surface. As indicated by the given geometric configurations for the intermediate points along MEP in Fig. 3, the states associated with the energy plateau are very similar to the end-on chemisorption state obtained in geometry optimization of (3×3)-Pt(111)/O_2/$H_9O_4^+$ system (Fig. 1B). The activation barrier for the transformation of end-on state to top-bridge-top state is ca. 0.05 eV.

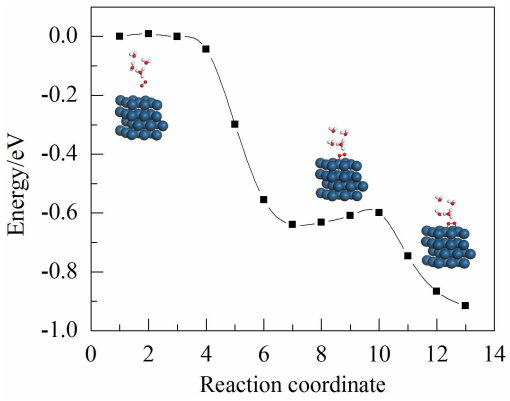

Fig. 3 The minimum energy paths for the transformations from physisorbed O_2 to the top-bridge-top adsorbed O_2 via the chemisorbed molecular O_2 of end-on configuration in the presence of hydrated proton $H_9O_4^+$

We also performed MEP analysis for direct dissociation of the end-on chemisorption state. As shown in Fig. 4, the activation barrier for this transformation is ca. 0.20 eV, which is very close to that for the dissociation of the top-bridge-top state. Thus, it is possible that the end-on chemisorption state may undergo a direct dissociation pathway.

In order to further examine the effect of oxygen coverage on ORR pathways, taking adsorption process of O_2 molecule as an example, the MEP analysis was performed for the transformation from physisorption state to top-bridge-top chemisorption

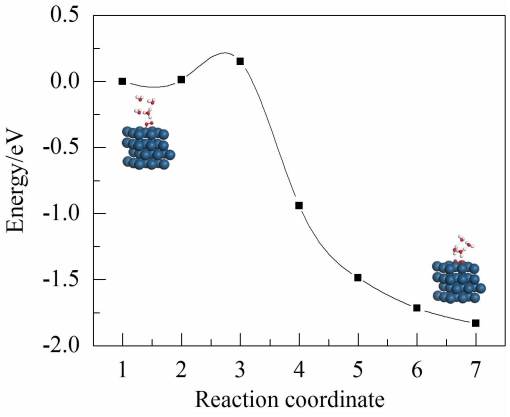

Fig. 4 The minimum energy paths for the transformations from the end-on adsorption state to dissociation in the presence of hydrated proton $H_9O_4^+$

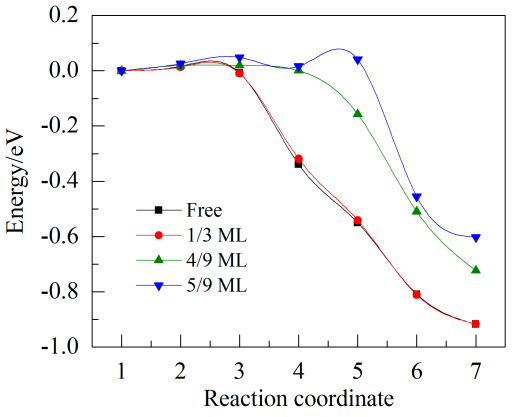

Fig. 5 The minimum energy paths for the transformation from physisorbed O_2 to the chemisorbed molecular O_2 of top-bridge-top configuration on the (3×3)-Pt (111) surface with different oxygen coverage(1/3 ML, 4/9 ML, and 5/9 ML) in the presence of hydrated proton $H_9O_4^+$

state on the (3×3)-Pt(111) surface with different numbers of pre-adsorbed oxygen atoms (O) in the presence of hydrated hydronium ion $H_9O_4^+$, as shown in Fig. 5. It can be seen that the reaction energy and activation barrier for this transformation change little when O coverage is 1/3 ML as compared with that on the (3×3)-Pt(111) surface without adding pre-adsorbed oxygen atoms. The activation barrier and the reaction energy show obvious changes only when oxygen coverage is increased to 5/9 ML. The values of -0.61 eV and 0.085 eV at this coverage are very close to that obtained on the (2×2)-Pt(111) surface (-0.61 eV and 0.13 eV respectively). This suggests that the change of slab size somewhat can mimic the effect of changing pre-adsorbed O in the calculation when investigating the oxygen coverage effect.

It should be pointed out that the electrode potential and proton concentration will be changed by using a different slab size. Moreover, along the reaction coordinate in Figs. 2-5, the electrode potential and proton concentration are not constant. So far, it remains a great challenge to perform MEP under constant potential control. Recently, Neurock et al.[18] and Liu et al.[19] have treated the effect of electrode potential in DFT calculations of electrochemical reaction paths by changing charge of reaction systems. The activation barriers in each reaction step were calculated under different charges and the optimal electro chemical reaction paths were determined under the charges which give same work function. This represents a significant advancement in modeling surface electrochemical processes. However, the results from this work function method remain of semi-quantitative significance when they are related to the experiments. First, the work function calculation of solvated surfaces in DFT frame is largely affected by the solvation conditions. In addition, it has considerable uncertainty when transferring the calculated work function to potential of hydrogen electrode scale since the exact work function of the latter is differently reported in the literature, from 4.4 eV to 4.8 eV. Therefore, attempt is not made to correct the varied potential effect in the present calculation. This makes the calculated activation barriers and reaction energies not quantitatively significant. However, they should still give the useful information on the sites and configuration for O_2 adsorption at the Pt/electrolyte interface, and the possible pathways of ORR and the effect of oxygen coverage. In addition, the similar adsorption intermediates obtained on slabs of different sizes suggest that the intermediate structures in ORR are not affected significantly by the proton concentration in acid media.

2) On the Use of Different Hydrated Proton Models

Ab initio molecular dynamics simulations indicate that two limiting proton structures exist: the Zundel structure ($H_5O_2^+$)[32] and the Eigen structure ($H_9O_4^+$)[33], and numerous other proton structures exist between these two limits[34]. The rationality of using $H_3O^+\cdots(H_2O)_2$ cluster ($H_7O_3^+$) to represent the solvation of proton in solution had been verified by the equilibrious structures of super-cell systems of Pt(111)/$H_3O^+\cdots(H_2O)_n$ and Pt(111)/O_2/$H_3O^+\cdots(H_2O)_n$ with n varying from 0 to 3 in our recent report[29], in which the proton can be reduced or specifically adsorbed on an uncharged Pt surface at Pt (111)/H_3O^+ interface, and the spontaneous proton transfer from the hydronium ion to Pt (111) surface can be prevented by replacing H_3O^+ with the Zundel cluster $H_3O^+\cdots H_2O$, $H_3O^+\cdots(H_2O)_2$, and Eigen cluster $H_3O^+\cdots(H_2O)_3$, implying that these hydrated hydronium ion can stabilize the proton at Pt/solution interface, whereas in geometry optimizations of Pt(111)/O_2/$H_3O^+\cdots(H_2O)_n$ systems, for $H_3O^+\cdots H_2O$, the optimization leads to a proton transfer from core hydronium ion to the chemisorbed oxygen molecule, forming a stable chemisorption state of bridge OOH*, This means that the Zundel cluster alone cannot stabilize the hydronium ion at O_2-adsorbed Pt/solution interface. To perform DFT calculations on these systems, a positive charge is introduced to the super-cells to form a hydrated proton. In the mean time, a homogeneous negative background charge of the same amount will be imposed automatically into the super-cells so that the entire periodic super-cell remains neural to avoid the divergence of Coulomb energy. It is known that the background charge will distort the distribution of electrostatic potential in the system and makes contribution to the DFT total energy. However, the geometric structures of the adsorbates at/near slab surface would not be substantially affected since the background charge mainly affects the potential distribution in the vacuum region[35].

A question may be asked whether the positive charge is added to the hydrated proton or it is distributed unifor mly in the super-cell. We have performed the Löwdin charge analysis on an isolated $H_7O_3^+$ and the Pt (111)/$H_7O_3^+$ system. It was found that the Löwdin charge of $H_7O_3^+$ in Pt(111)/$H_7O_3^+$ system is ca. 23.7733 electrons, which is very close to the calculated Löwdin charge for the isolated $H_7O_3^+$ (23.7667 electrons). This makes us believe that the charge will be added to the hydrated proton, which will be energetically more favored than uniformly distributing the charge in entire super-cell system.

The adsorption property of the surface species forming hydrogen bond with H_2O molecules can be affected by solvent environment[36-37]. Thus, in present study, we consider the solvent effect on hydrated proton model. The most accurate way of including the effect of water is to explicitly add water molecules with sufficient quantity into the simulations. At temperatures and pressures relevant for an electrochemical experiment, the water-containing electrolyte will be liquid. However, since in this context we are mainly interested in the effect of different hydrated ion models on DFT calculation of ORR pathways and not so much the actual structural of liquid water itself, we can probably simplify the problem by additionally adding a water bilayer around the hydrated proton. The water bilayer on Pt(111) has been used extensively in DFT calculation study of surface electrochemical processes[37-38]. The advantage of using the bilayer structure of H_2O molecules to model solvent effect lies in that the model only requires limited amounts and well-defined structure of H_2O molecules. However, it should be pointed out that it is still not clear whether the water bilayer structure is thermodynamically stable or not at temperatures and pressures relevant for an electrochemical experiment[39].

In order to further confirm the stability of bare H_3O^+, we added additional bilayer structure of H_2O molecules in Pt(111)/H_3O^+ system in present study. As shown in Fig. 6A, the geometry optimization of "Pt/H_3O^+" system produces similarly an adsorbed hy

drogen and a water molecule on the Pt(111) surface, such an instability of the bare H_3O^+ at Pt(111)/H_3O^+ interface was also shown by Hyman and Medlin [6]. This seems to imply that the bare H_3O^+ is instable even if the presence of bilayer structure of H_2O molecules, namely, using the bare H_3O^+ to simulate hydrated hydronium ion is inappropriate. A top-bridge-top configured chemisorption state of O—O* is obtained without obvious proton transfer occurring via the geometry structure optimization of Pt(111)/O_2/$H_3O^+\cdots$ $(H_2O)_n$ with n varying from 1 to 3 in the presence of bilayer structure of H_2O structure (as shown in Fig. 6B-D), indicating that $H_5O_2^+$, $H_7O_3^+$, and $H_9O_4^+$ all can stabilize the proton therein.

However, the dissociation adsorbed state obtained from $H_5O_2^+$ is inconsistent with that obtained from $H_7O_3^+$ and $H_9O_4^+$. Adsorbed O atom at fcc hollow site and adsorbed OH species at top site are formed on the Pt(111) surface when using $H_5O_2^+$ model (as shown in Fig. 7A), whereas two adsorbed O atoms are obtained at fcc hollow sites when using $H_7O_3^+$ or $H_9O_4^+$ (as shown in Fig. 7B-C). Therefore, proton cannot be stabilized by $H_5O_2^+$ model even if considering additional solvent effect. These results provide further support for the rationality to use $H_7O_3^+$ and $H_9O_4^+$ to represent the hydration interaction of proton in acid solution for DFT calculation of ORR pathways.

The effect of hydrated proton model on DFT calculations of ORR pathways on the Pt(111) surface was further validated. Similarly, taking adsorption process of O_2 molecule as an example, the MEP analysis was performed for the transformation from physisorption state to the chemisorbed molecular O_2 of top-bridge-top configuration on the (2×2)-Pt(111) surface in the presence of hydrated proton $H_9O_4^+$, which has been studied using hydrated proton model $H_7O_3^+$ in our previous paper[29-30]. As shown in Fig. 8, the reaction energy and activation barrier when using hydrated proton $H_9O_4^+$ are ca. -0.68 and 0.084 eV, respectively, which are very close to the value of corresponding process when using hydrated proton $H_7O_3^+$. Thus, the results provide further support for the rationality to use $H_7O_3^+$ and $H_9O_4^+$ to represent the hydrated proton model in acid solution for studying the ORR pathways based on DFT calculation, and the effect of both these hydrated proton models on DFT calculations of ORR pathways is not significant. In the mean time, we scrutinized carefully the MEP, and an intermediate of end-on chemisorption state was found. Thus, the result also supports the conclusion of the above analysis that a relatively stable end-on adsorbed intermediate is formed in course of the formation of top-bridge-top chemisorption state. Additionally, the reaction energy and activation barrier on the (2×2)-Pt(111) surface when using hydrated proton $H_9O_4^+$ are also very close to that of corresponding process on the (3×3)-Pt(111) surface with oxygen

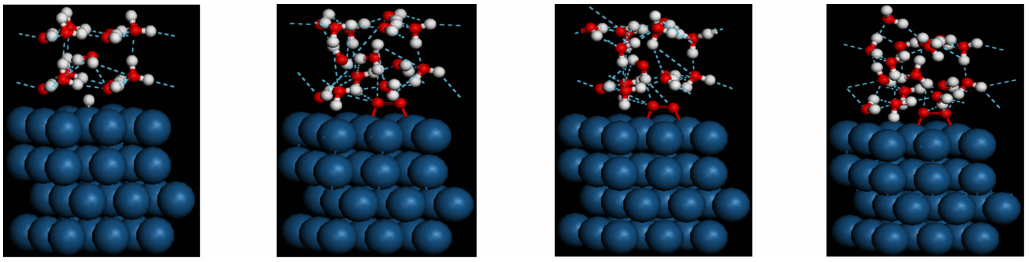

Fig. 6 The optimized structures of chemisorption state of Pt(111)/H_3O^+ and Pt(111)/O_2/$H_3O^+\cdots(H_2O)_n$ super-cell systems in the presence of the H_2O bilayer: A. H_3O^+; B. $H_5O_2^+$-O_2; C. $H_7O_3^+$-O_2; D. $H_9O_4^+$-O_2

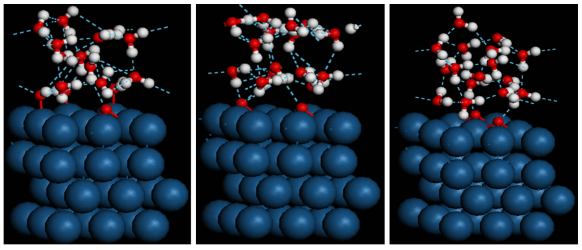

Fig. 7 The optimized structures of dissociation adsorbed state of $Pt(111)/O_2/H_3O^+\cdots(H_2O)_n$ super-cell systems: A. H_5O_2-O_2; B. $H_7O_3^+$-O_2; C. $H_9O_4^+$-O_2

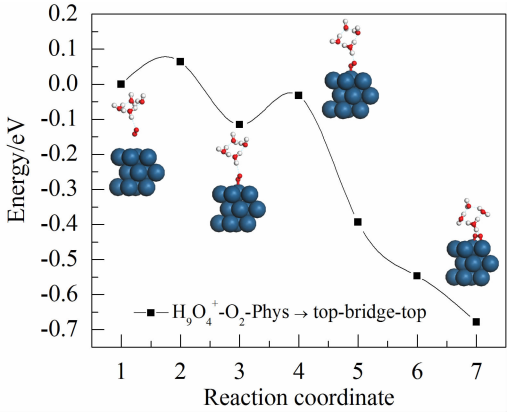

Fig. 8 The minimum energy paths for the transformations from physisorbed O_2 to the chemisorbed molecular O_2 of top-bridge-top configuration on the (2×2)-Pt(111) surface in the presence of hydrated proton $H_9O_4^+$

coverage of 5/9 ML, the results further confirm the effect of oxygen coverage on ORR mechanisms.

2.2 Serial Protonation of Dissociative Products

The abovementioned results indicate that the adsorption and dissociation process is almost non-activated on the (3×3)-Pt(111) surface. In order to validate the degree of difficulty in dissociative products further reduction, we performed MEP analysis for the protonation of O and OH species using CI-NEB method, respectively. As shown in Fig. 9, the activation barriers need to be overcome by O protonation to form OH and by OH protonation to form H_2O are 0.85 and 0.07 eV, respectively. This finding indicated that the activation barriers of these two protonation processes are higher than those of adsorption and dissociation process as previously mentioned.

Based on above analysis and our previous report, the results may be able to give two possible four-electron ORR pathways on the (2×2) and on the (3×3)-Pt(111) surfaces, respectively, see Tab. 2. However, these ORR pathways may be not accurate completely due to the drawbacks of computational methods. In these both ORR pathways under different oxygen coverages, the chemisorbed state dissociated to form O and OH species under high oxygen coverage, whereas two dissociative adsorbed O atoms were formed under low oxygen coverage. The reason for the difference may lie in that high oxygen coverage makes O atoms more attractive to hydrated hydronium ion, thus leading to the formation of OH species.

The activation barriers of each step in both ORR pathways are also summarized in Tab. 2. It can be seen that the *rds* may be the reaction that O atom protonation formed OH species on the Pt(111) surfaces under different oxygen coverage and hydrated proton model, which can explain well why Pt-based alloy catalysts of weak adsorbed oxygen species were excellent ORR catalysts[40]. Recently, Nørskov et al.[41] theoretically and experimentally investigated metallic ORR catalysts made from alloys. The results demonstrated that new and excellent ORR electrocatalytic materials such as Pt_3Sc and Pt_3Y alloys can be found, and that theoretical work can effectively support the search for improved catalytic materials, in which the oxygen species are more weakly adsorbed onto Pt_3Sc and Pt_3Y alloys than on pure Pt surface. Regarding other Pt-based alloy catalysts binding atomic oxygen more weakly, calculations have also predicted that PtM (M = Fe, Co, Ni, etc.) alloys should have higher catalytic activity than pure Pt, which has also been experimentally proven[40, 42-46].

Comparison in the activation barriers of the ORR pathways showed that the adsorption and dissociation process of O_2 molecule may easily occur by the thermo-active process regardless of being high or low oxygen coverage although the activation barriers for O_2 adsorption and dissociation on the (2×2)-Pt(111) surface are slightly higher than those on the (3×3)-Pt(111) surface. For the serial protonation process of the dis

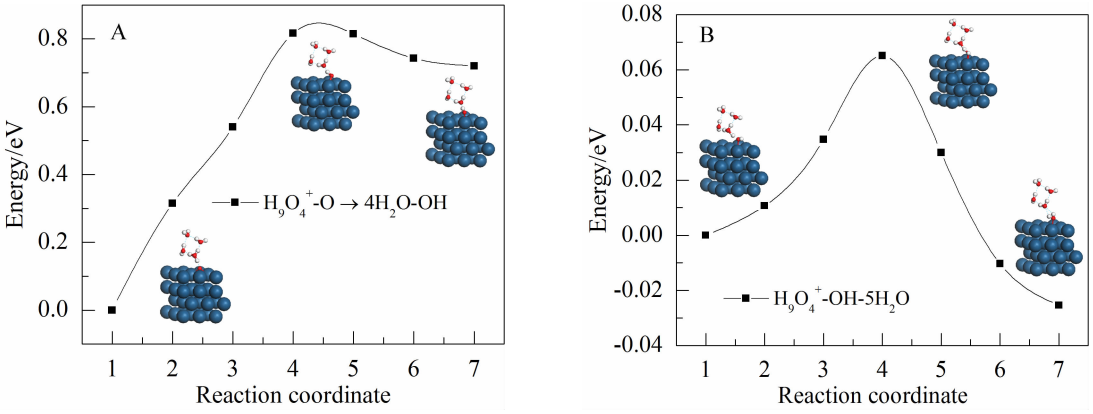

Fig. 9 The minimum energy paths for the protonation of O to form OH (A) and OH to form H_2O (B)

Tab. 2 Two possible four-electron ORR pathways on the (2×2) and (3×3)-Pt(111) surfaces

Surface	The possible dissociation pathway of O_2 Molecule	The possible dissociation pathway of OOH species	Activation barrier/eV
(2×2)-Pt(111)/$O_2H_7O_3^+$	$O_2 \rightarrow O_{2ad}$	$O_2 + H^+ + e \rightarrow OOH_{ad}$	-0.13
	$O_{2ad} + H^+ + e \rightarrow O_{ad} + OH_{ad}$	$OOH_{ad} \rightarrow O_{ad} + OH_{ad}$	
	$O_{ad} + H^+ + e \rightarrow OH_{ad}$	$O_{ad} + H^+ + e \rightarrow OH_{ad}$	0.56
	$2OH_{ad} + 2H^+ + 2e \rightarrow 2H_2O_{ad}$	$2OH_{ad} + 2H^+ + 2e \rightarrow 2H_2O_{ad}$	0.29
(3×3)-Pt(111)/$O_2H_9O_4^+$	$O_2 \rightarrow O_{2ad}$	$O_2 + H^+ + e \rightarrow OOH_{ad}$	-0.02
	$O_{2ad} \rightarrow O_{ad} + O_{ad}$	$OOH_{ad} \rightarrow O_{ad} + H^+ + e$	
	$2O_{ad} + 2H^+ + 2e \rightarrow 2OH_{ad}$	$2O_{ad} + 2H^+ + 2e \rightarrow 2OH_{ad}$	0.85
	$2OH_{ad} + 2H^+ + 2e \rightarrow 2H_2O_{ad}$	$2OH_{ad} + 2H^+ + 2e + 2H_2O_{ad}$	0.07

sociative products to form H_2O molecule, the activation barriers needed to be overcome by O protonation to form OH and by OH protonation to form H_2O are 0.56 and 0.29 eV on the (2×2)-Pt(111) surface, respectively. By contrast, the activation barriers of the same processes are 0.85 and 0.07 eV on the (3×3)-Pt(111) surface, respectively, indicating that the protonation process of OH species to form H_2O molecule may more easily occur on the Pt(111) surface with low oxygen coverage. However, the activation barriers for the process of O atom protonation to form OH species become larger on the (3×3)-Pt(111) surface. Larger activation energy for this process explains why the chemisorbed state dissociated to form O and OH species on the Pt(111) surface with high oxygen coverage, whereas two adsorbed O atoms are formed on the Pt (111) surface with low oxygen coverage during geometry optimization. Simultaneously, The reason for larger activation energy may be that weaker repulsive interaction among adsorbed O atoms on the Pt(111) surface with low oxygen coverage leads to stronger adsorption of O atoms, thus, it is more difficult for further O protonation to form OH species on the Pt(111) surface with low oxygen coverage compared with that under high oxygen coverage. Additionally, the reaction energy is 0.72 eV for the process of O atom protonation to form OH species on the (3×3)-Pt(111) surface, it is more positive than that of the corresponding process (0.50 eV) on the (2×2)-Pt(111) surface. Based on the BEP relationship, the larger activation energy for this process on the Pt(111) surface with low oxygen coverage could be also explained.

The findings will lead to a deeper understanding of ORR and can provide a theoretical basis for designing Pt-based alloy catalysts of ORR in fuel cells. As reported in our previous work[29], the effect of zero point energies is insignificant and does not alter the trends of reaction path regardless of being in the gas phase or in the presence of hydrated hydronium ion. Thus, the effect of zero point energies on reaction paths has not been considered in present work.

3 Conclusions

The effects of oxygen coverage and hydrated proton model on the DFT calculations of ORR pathways on the Pt(111) surface have been studied. It is shown that the use of different hydrated proton models does not change the calculated pathways. The formation of aprotonated end-on chemisorbed state of OOH* is likely the first step of ORR on the Pt(111) surface regardless of the oxygen coverage. The MEP calculations on various possible steps suggest that the protonation of O* to form OH* species may be the *rds* in the ORR regardless of the O* coverage, which may explain why catalysts that bind atomic oxygen more weakly have better ORR activity. With increased oxygen coverage, the activation energy of the *rds* decreases. Thus, The ORR activity should be strongly coverage-dependent.

References:

[1] Nilekar A U, Mavrikakis M. Improved oxygen reduction reactivity of platinum monolayers on transition metal surfaces[J]. Surface Science, 2008, 602(14): L89-L94.

[2] Janik M J, Taylor C D, Neurock M. First-principles analysis of the initial electroduction steps of oxygen over Pt (111) [J]. Journal of the Electrochemical Society, 2009, 156(1): B126-B135.

[3] Panchenko A, Koper M T M, Shubina T E, et al. *Ab initio* calculations of intermediates of oxygen reduction on low-index platinum surfaces[J]. Journal of the Electrochemical Society, 2004, 151(12): A2016-A2027.

[4] Neyerlin K C, Gu W, Jorne J, et al. Determination of catalyst unique parameters for the oxygen reduction reaction in a PEMFC[J]. Journal of the Electrochemical Society, 2006, 153(10): A1955-A1963.

[5] Sidik R A, Anderson A B. Density functional theory study of O_2 electroreduction when bonded to a Pt dual site [J]. Journal of Electroanalytical Chemistry, 2002, 528 (1/2): 69-76.

[6] Hyman M P, Medlin J W. Mechanistic study of the electrochemical oxygen reduction reaction on Pt (111) using den sity functional theory[J]. The Journal of Physical Chemistry B, 2006, 110(31): 15338-15344.

[7] (a) Wang Y X, Balbuena P B. *Ab initio* molecular dynamics simulations of the oxygen reduction reaction on a Pt(111) surface in the presence of hydrated hydronium $(H_3O)^+(H_2O)_2$: Direct or series pathway[J]. The Journal of Physical Chemistry B, 2005, 109 (31), 14896-14907; (b) Wang Y, Balbuena P B. Roles of proton and electric field in the electroreduction of O_2 on Pt(111) surfaces: Results of an ab-initio molecular dynamics study[J]. The Journal of Physical Chemistry B, 2004, 108(14): 4376-4384.

[8] Qi L, Yu J G, Li J. Coverage dependence and hydroperoxyl-mediated pathway of catalytic water formation on Pt(111) Surface [J]. The Journal of Chemical Physics, 2006, 125(5): 054701.

[9] Zhang T, Anderson A B. Oxygen reduction on platinum electrodes in base: Theoretical study[J]. Electrochimica Acta, 2007, 53(2): 982-989.

[10] Jocob T, Goddard W A. Water formation on Pt and Pt-based alloys: A theoretical description of a catalytic reaction[J]. ChemPhysChem, 2006, 7(5): 992-1005.

[11] Wang J X, Zhang J L, Adzic R R. Double-trap kinetic equation for the oxygen reduction reaction on Pt(111) in acidic media[J]. The Journal of Physical Chemistry A, 2007, 111(49): 12702-12710.

[12] Yeager E, Razaq M, Gervasio D, et al. The electrolyte factor in O_2 reduction electrocatalysis[C]//Proceedings of the workshop on structural effects in electrocatalysis and oxygen electrochemistry. Pennington, NJ: The Electrochemical Society, 1992: 440.

[13] (a) Damjanovic A, Brusic V, Bockris J O M. Mechanism of oxygen reduction related to electronic structure of gold-palladium alloy[J]. The Journal of Physical Chemistry, 1967, 71 (8): 2741-2742; (b) Damjanovic A, Brusic V. Electrode kinetics of oxygen reduction on oxide-free platinum electrodes[J]. Electrochimica Acta, 1967, 12(6): 615-628.

[14] Damjanovic A. Progress in the studies of oxygen reduction during the last thirty years[M]//Murphy O J, Srinivasan S, Conway B E, Eds. Electrochemistry in Transition. New York: Plenum Press, 1992: 107.

[15] Sha Y, Yu T H, Liu Y, et al. Theoretical study of solvent effects on the platinum-catalyzed oxygen reduction reaction[J]. The Journal of Physical Chemistry Letters, 2010,

1(5): 856-861.

[16] Tripkovic V, Skulason E, Siahrostami S, et al. The oxygen reduction reaction mechanism on Pt(111) from density functional theory calculations[J]. Electrochimica Acta, 2010, 55(27): 7975-7981.

[17] Sha Y, Yu T H, Merinov B V, et al. Mechanism for oxygen reduction reaction on Pt_3Ni alloy fuel cell cathode[J]. The Journal of Physical Chemistry C, 2012, 116 (45): 21334-21342.

[18] Filhol J S, Neurock M. Elucidation of the electrochemical activation of water over Pd by first principles[J]. Angewandte Chemie International Edition, 2006, 45(3): 402-406.

[19] Wei G F, Fang Y F, Liu Z P. First principles tafel kinetics for resolving key parameters in optimizing oxygen electrocatalytic reduction catalyst[J]. The Journal of Physical Chemistry C, 2012, 116(23): 12696-12705.

[20] Perdew J P, Burke K, Ernzerhof M. Generalized gradient approximation made simple[J]. Physical Review Letters, 1996, 77(18): 3865-3868.

[21] Vanderbilt D. Soft self-consistent pseu dopotentials in a generalized eigenvalue formalism[J]. Physical Review B, 1990, 41(11): 7892-7895.

[22] Methfessel M, Paxton A T. Soft self-consistent pseudopotentials in a generalized eigenvalue formalism[J]. Physical Review B, 1989, 40(6): 3616-3621.

[23] Baroni S, Dal Corso A, de Gironcoli S, et al. PWSCF and PHONON: Plane-wave pseudo-potential codes[OL]. http://www.pwscf.org, 2001.

[24] Kokalj A. XCrySDen—A new program for displaying crystalline structures and electron densities[J]. Journal of Molecular Graphics and Modelling, 1999, 17(3): 176-179.

[25] Kokalj A, Causa M. Scientific visualization in computational quantum chemistry[C]//Proceedings of high performance graphics systems and applications european workshop. Bologna, Italy: CINECA-Interuniversity Consortium, 2000.

[26] Kokalj A, Causà M. XCrySDen: (*X*-Window) CRYstalline structures and DENsities[OL]. http://www-k3.ijs.si/kokalj/xc/XCrySDen.html, 2001.

[27] Henkelman G, Jonsson H. Improved tangent estimate in the nudged elastic band method for finding minimum energy paths and saddle points[J]. The Journal of Chemical Physics, 2000, 113(22): 9978-9985.

[28] Henkelman G, Uberuaga B P, Jonsson H. A climbing image nudged elastic band method for finding saddle points and minimum energy paths[J]. The Journal of Chemical Physics, 2000, 113(22), 9901-9904.

[29] Ou L H, Yang F, Liu Y W, et al. First-principle study of the adsorption and dissociation of O_2 on Pt(111) in acidic media[J]. The Journal of Physical Chemistry C, 2009, 113(48): 20657-20665.

[30] Ou L H, Chen S L. Comparative study of oxygen reduction reaction mechanisms on the Pd(111) and Pt(111) surfaces in acid medium by DFT[J]. The Journal of Physical Chemistry C, 2013, 117(3): 1342-1349.

[31] Bligaard T, Nørskov J K, Dahl S, et al. The Brønsted-Evans-Polanyi relation and the volcano curve in heterogeneous catalysis[J]. Journal of Catalysis, 2004, 224(1): 206-217.

[32] Zundel G. In the hydrogen bonds recent developments in theory and experiments [M]//Schuster P, Zundel G, Sandorfy C, Eds. II. Structure and spectroscopy. Amsterdam: North-Holland Publishing Company, 1976: 683-766.

[33] Eigen M. Proton transfer, acid-base catalysis, and enzymatic hydrolysis. Part I: elementary processes [J]. Angewandte Chemie International Edition, 1964, 3(1): 1-19.

[34] Marx D, Tuckerman M E, Hutter J, et al. The nature of the hydrated excess proton in water[J]. Nature, 1999, 397 (6720): 601-604.

[35] (a) Lozovoi A, Alavi A, Kohanoff J, et al. *Ab initio* simulation of charged slabs at constant chemical potential[J]. The Journal of Chemical Physics, 2001, 115(4): 1661-1669; (b) Filhola J S, Bocquet M L. Charge control of the water monolayer/Pd interface[J]. Chemical Physics Letters, 2007, 438(4-6): 203-207.

[36] Thiel P A, Madey T E. The interaction of water with solid surfaces-fundamental aspects[J]. Surface Science Reports, 1987, 7(6/8): 211-385.

[37] Henderson M A. Interaction of water with solid surfaces: Fundamental aspects revisited[J]. Surface Science Reports, 2002, 46(1/8): 5-308.

[38] Ogasawara H, Brena B, Nordlund D, et al. Structure and bonding of water on Pt(111)[J]. Physical Review Letters, 2002, 89(27): 276102.

[39] (a) Schnur S, Groβ A. Properties of metal–water interfaces studied from first principles[J]. New Journal of Physics, 2009, 11(12): 125003; (b) Roudgar A, Groβ A. Water bilayer on the Pd/Au(111) overlayer system: Coadsorption and electric field effects[J]. Chemical Physics Letters, 2005, 409(4/6): 157-162.

[40] Nørskov J K, Rossmeisl J, Logadotir A, et al. Origin of the overpotential for oxygen reduction at a fuel-cell cathode[J]. The Journal of Physical Chemistry B, 2004, 108 (46): 17886-17892.

[41] Greeley J, Stephens I E L, Bondarenko A S, et al. Alloys

of platinum and early transition metals as oxygen reduction electrocatalysts[J]. Nature Chemistry, 2009, 1(7): 552-556.

[42] Mazumder V, Chi M F, More K L, et al. Synthesis and characterization of multimetallic Pd/Au and Pd/Au/FePt core/shell nanoparticles[J]. Angewandte Chemie International Edition, 2010, 49(49): 9368-9372.

[43] Stamenkovic V, Fowler B, Mun B S, et al. Improved oxygen reduction activity on $Pt_3Ni(111)$ via increased surface site availability[J]. Science, 2007, 315(5811): 493-497.

[44] Koh S, Strasser P. Electrocatalysis on bimetallic surfaces: Modifying catalytic reactivity for oxygen reduction by voltammetric surface dealloying[J]. Journal of the American Chemical Society, 2007, 129(42): 12624-12625.

[45] Chen S, Sheng W C, Yabuuchi N, et al. Origin of oxygen reduction reaction activity on "Pt_3Co" nanoparticles: Atomically resolved chemi cal compositions and structures[J]. The Journal of Physical Chemistry C, 2009, 113 (3): 1109-1125.

[46] Wakisaka W, Suzuki H, Mitsui S, et al. Increased oxygen coverage at Pt-Fe alloy cathode for the enhanced oxygen reduction reaction studied by EC-XPS[J]. The Journal of Physical Chemistry C, 2008, 112 (7): 2750-2755.

基于 DFT 计算的 Pt(111)表面氧覆盖度和水合质子模型对氧还原反应路径的影响

欧利辉[1,2], 陈胜利[2*]

(1. 湖南文理学院化学化工学院,湖南 常德 415000; 2. 武汉大学化学与分子科学学院,湖北 武汉 430072)

摘要: 利用基于平面波的密度泛函理论(DFT)计算研究了氧气分子在 Pt(111)表面的吸附和解离,以及解离产物进一步质子化形成 H_2O 的过程. 通过使用不同尺寸的平板模型和在表面预吸附不同数量的氧原子, 研究了氧覆盖度对氧还原反应(ORR) 路径的影响, 并对使用不同水合质子模型的计算结果进行了比较. 研究结果表明: 质子化的 end-on 化学吸附态 OOH* 的形成是 ORR 的初始步骤;OOH* 能够转化形成非质子化的 top-bridge-top 化学吸附态 O_2*, 或者解离形成吸附的 O* 物种. 对不同氧覆盖度下各种可能步骤的活化能计算结果表明,O* 的质子化形成 OH* 物种是 ORR 的速决步骤. 增加氧覆盖度时,该步骤的活化能减少. 此外,还发现使用比 $H_7O_3^+$ 更复杂的水合质子模型不会改变计算所得的反应路径.

关键词: 最小能量路径; ORR 机理; 氧覆盖度; 水合质子模型